



UNIVERSIDADE ESTADUAL DE CAMPINAS
SISTEMA DE BIBLIOTECAS DA UNICAMP
REPOSITÓRIO DA PRODUÇÃO CIENTÍFICA E INTELLECTUAL DA UNICAMP

Versão do arquivo anexado / Version of attached file:

Versão do Editor / Published Version

Mais informações no site da editora / Further information on publisher's website:

<https://journals.aps.org/prl/abstract/10.1103/PhysRevLett.97.155501>

DOI: 10.1103/PhysRevLett.97.155501

Direitos autorais / Publisher's copyright statement:

©2006 by American Physical Society. All rights reserved.

DIRETORIA DE TRATAMENTO DA INFORMAÇÃO

Cidade Universitária Zeferino Vaz Barão Geraldo

CEP 13083-970 – Campinas SP

Fone: (19) 3521-6493

<http://www.repositorio.unicamp.br>

Structure and Energetics of Molecular Point Defects in Ice I_h

Maurice de Koning,^{1,*} Alex Antonelli,¹ Antonio J. R. da Silva,² and A. Fazzio²

¹*Instituto de Física Gleb Wataghin, Universidade Estadual de Campinas, Unicamp,
Caixa Postal 6165, 13083-970, Campinas, São Paulo, Brazil*

²*Instituto de Física, Universidade de São Paulo, Caixa Postal 66318, 05315-970, São Paulo, São Paulo, Brazil*

(Received 31 May 2006; published 9 October 2006)

We present a first-principles study of the molecular vacancy and three distinct molecular interstitial structures in ice I_h . The results indicate that, due to its bonding to the surrounding hydrogen-bond network, the bond-center (Bc) configuration is the favored molecular interstitial in ice I_h . A comparison between the vacancy and the Bc interstitial suggests that the former is the predominant molecular point defect for $T \lesssim 200\text{K}$ although a crossover scenario in which the latter becomes favored below the melting point is conceivable.

DOI: [10.1103/PhysRevLett.97.155501](https://doi.org/10.1103/PhysRevLett.97.155501)

PACS numbers: 61.72.Ji, 31.70.Ks, 71.15.Mb

While the proton-disordered ice I_h is one of the most abundant crystalline solids on Earth, our understanding of many of its properties remains incomplete [1]. An important aspect in this regard involves the comprehension of the role of crystal defects and it is remarkable that not even the most basic disruptions of crystalline order, the molecular vacancy, and self-interstitial, are well understood [1]. Since they are involved in diffusion and possibly affect the electrical properties of ice I_h [1,2], the central issue revolves around the questions: which of the two is the primary molecular point-defect species, and what is its structure [1]?

From the experimental side, positron annihilation experiments [3,4] first indicated that the vacancy should be overall dominant, but a more recent series of x-ray topographical studies of dislocation loops [5–9] provided convincing evidence that for $T \gtrsim -50^\circ\text{C}$ the self-interstitial should take over. The structure of this self-interstitial, however, remains unknown. In addition to a surprisingly high formation entropy of $\sim 4.9k_B$, the x-ray studies inferred a formation energy below the sublimation energy of ice I_h , which led to the suggestion [5] that its structure might involve bonding to the surrounding hydrogen-bond network. This idea, however, contrasts with the established consensus [1] that the relevant structures involve the two cavity-centered positions, i.e., the capped (Tc) and uncapped (Tu) trigonal sites [1], for which such bonding is not expected [1,10]. The theoretical insight from classical molecular dynamics (MD) simulations [11–13] has also been largely inconclusive, mostly due to the sensitivity of the results to the choice of water model.

In this Letter we present a density-functional-theory (DFT) *ab initio* study in which we investigate the structure and formation free energies of three self-interstitial configurations and the molecular vacancy in ice I_h , and compare the corresponding thermal-equilibrium concentrations. Following recent studies involving defects in ice I_h , [14] our calculations are performed using the VASP package [15,16], employing the Perdew-Wang 91

generalized-gradient approximation and the projector-augmented-wave [17] approach. We utilize a 96-molecule proton-disordered supercell [18], restrict Brillouin-zone sampling to the Γ point, and adopt a plane-wave cutoff of 700 eV. To consider effects related to thermal expansion we carry out the calculations for three sets of lattice parameters, chosen to correspond to their zero-pressure experimental values [1] at 10, 205, and 265 K, respectively. To sample the influence of the proton-disorder, which causes random local environments for each defect, we study a number of different realizations of each defect type, positioning a given defect at a number of different sites in the defect-free cell. In addition, for the self-interstitial defects we also consider the possibility of multiple orientations of the interstitial molecule on a given defect site.

Figure 1 shows typical optimized structures of the three investigated interstitial structures, obtained after relaxation of all atomic degrees of freedom at constant (defect-free crystal) volume. Formation-volume effects are not expected to significantly affect formation energies [19]. Panels (a) and (b) show the Tc and Tu interstitial structures, respectively. Both are similar in that neither significantly disrupts the surrounding hydrogen-bond network and both resemble isolated water molecules, with covalent O-H bond lengths $\sim 3\%$ shorter than in bulk ice. The structure of the interstitial shown in panel (c) differs fundamentally from these two. Its formation involves the breaking of a hydrogen bond between the bulk molecules 1 and 2, followed by the creation of two new ones in which the interstitial molecule accepts and donates a proton from or to the molecules 1 and 2, respectively, incorporating the molecule into the surrounding hydrogen-bond network. This bond-center (Bc) interstitial structure resembles a configuration observed in one of the recent MD simulations [13], although no detailed structural nor energetics data were reported. The hydrogen bonds in the vicinity of the defect are predominantly compressed, with O-O distances up to 5% shorter compared to the typical value in

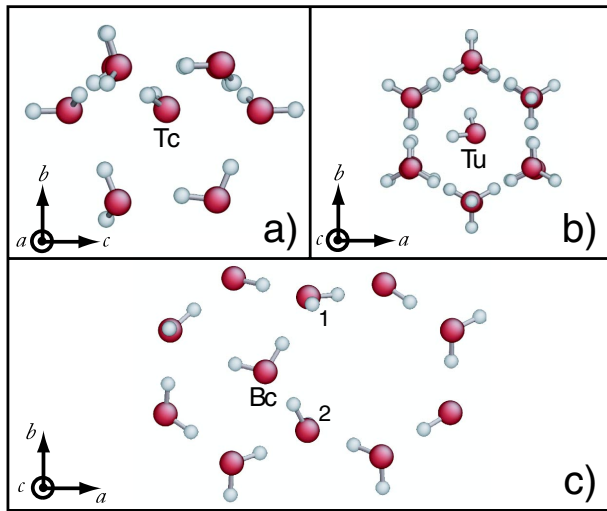


FIG. 1 (color online). Typical realizations of investigated molecular interstitial structures in ice I_h . Arrows indicate crystallographic directions (cf. Ref. [1]). (a) Capped trigonal (Tc) interstitial. (b) Uncapped trigonal (Tu) interstitial. (c) Bond-center (Bc) interstitial.

defect-free ice I_h . The creation of a molecular vacancy (not shown) involves the breaking of four hydrogen bonds, leaving two dangling covalent O-H bonds. In contrast to the Bc interstitial the majority of the hydrogen bonds near the vacancy are stretched, with O-O distances up to 3% longer than in the defect-free crystal.

To obtain insight into the relative stability of these defects we compute their formation free energies as a function of temperature. Using the relaxed structures for the defect-free and defected cells, we first compute the DFT total-energy contributions using 8 different realizations for the Tu and Bc interstitials, sampling 5 different sites in the cell, as well as 3 distinct molecular orientations at one particular site. For the vacancy we considered 6 distinct defect sites and, in view of its elevated formation energy, only one realization was considered for the Tc interstitial. The results are presented in Fig. 2(a), which shows the DFT formation energies averaged over the different realizations of each defect, as a function of the temperature corresponding to the experimental lattice parameter values used in the calculations.

The DFT formation energy of the Tc interstitial is by far the highest among the four point-defect species and it is not expected to be relevant as a thermal-equilibrium defect in ice. Although the formation energy of the Tu interstitial is around 0.2 eV lower than that of the Tc interstitial, it is significantly larger than that of the Bc interstitial and molecular vacancy. Comparing the latter two, although having essentially equal formation energies at low temperatures, it is found that the Bc interstitial is particularly sensitive to thermal expansion, showing a reduction of $\sim 7\%$ upon a linear lattice expansion of only $\sim 0.5\%$. This effect is visibly less pronounced for the vacancy,

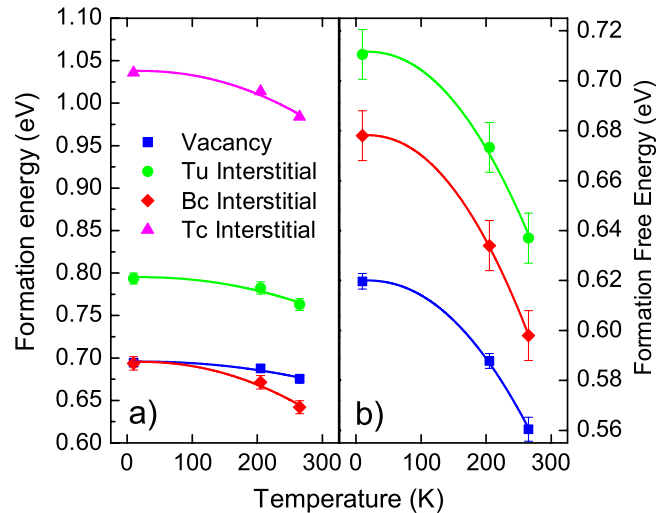


FIG. 2 (color online). (a) DFT formation energies as a function of temperature for the Tc interstitial (Δ), Tu interstitial (\circ), Bc interstitial (\diamond), and vacancy (\square), averaged over different realizations. (b) Average local-harmonic formation free energies of Tu interstitial (\circ), Bc interstitial (\diamond), and vacancy (\square). Error bars in (a) and (b) represent standard deviations in the mean values.

which shows a decrease of only $\sim 2\%$. A comparison between both defects suggests that the strengthened bonding of the Bc interstitial is associated with the relief of compressed hydrogen bonds upon thermal expansion. Since almost all the hydrogen bonds in the vicinity of the Bc interstitial are compressed, this effect is expected to be stronger than for the vacancy, for which only a third of the affected hydrogen bonds are compressed.

To compute the total formation free energies of the defects, we need to include zero-point and finite-temperature vibrational contributions. To this end, we apply the local-harmonic approximation [20], in which these effects are taken into account by comparing the local vibrational modes of the molecules in the presence of the defect to those in the defect-free configuration. For this purpose we consider only the molecules showing significant distortions compared to the defect-free lattice, restricting the analysis to molecules within the second-nearest neighbor shell of the defect. We compute the inter- and intramolecular vibrational frequencies by numerically estimating the rigid-molecule force and torque constants as well as the force constants associated with the internal degrees of freedom, followed by the diagonalization of the corresponding local dynamical matrices. Given the high DFT formation energy of the Tc interstitial and the elevated computational cost we restrict this analysis to single realizations of the molecular vacancy and the Tu and Bc interstitials.

The results for $T = 10$ K are displayed in Fig. 3. Each data point represents a particular vibrational mode ν , whose energy in the defect-free cell is plotted on the

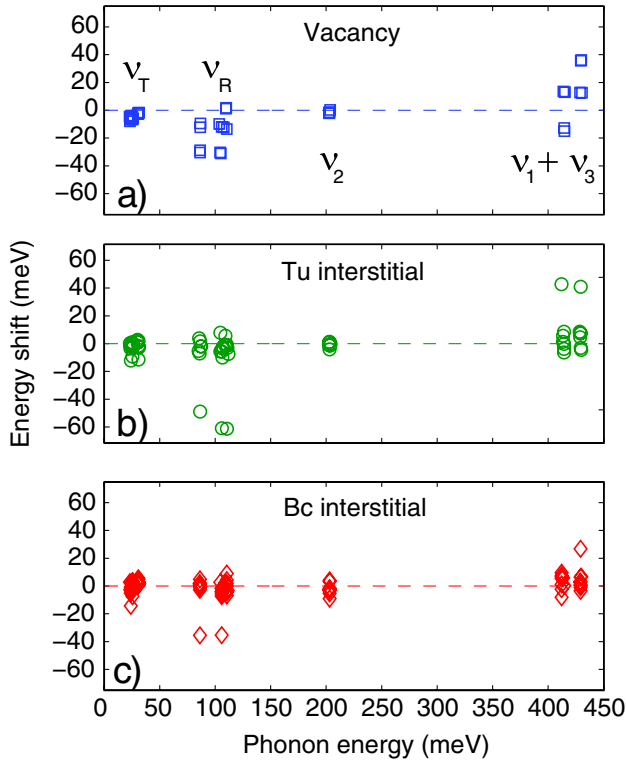


FIG. 3 (color online). Vibrational frequency shifts due to the presence of the three point defects. Horizontal axis describes the energy $h\nu$ of each vibrational mode in the defect-free crystal. Vertical axis describes the energy shift in the presence of the defect. Panel (a) vacancy, (b) Tu interstitial, (c) Bc interstitial. Symbols ν_T , ν_R , ν_2 , and $\nu_1 + \nu_3$ denote, respectively, groups of molecular translational, molecular librational, intramolecular bending, and intramolecular stretching modes, cf. Ref. [1].

horizontal axis. The vertical axis then describes how it changes in the presence of the defect. The perfect-crystal vibrational modes can be divided into four groups, which, respectively, correspond to the molecular translational, molecular librational, intramolecular bending, and intramolecular stretching modes. The energies of the four groups are in excellent agreement with experimental inelastic neutron scattering data [21]. Considering the influence of the point defects, their presence mostly affects two groups, causing softening of molecular librational modes and stiffening of intramolecular stretching modes while the molecular translational and intramolecular bending modes remain largely unaltered. These frequency shifts are related to the partially hydrogen-bonded molecules in the defect region, with the stiffening revealing free-molecule-like O-H bonds and the softening indicative of weakened hydrogen bonds. The temperature dependence of the frequencies, investigated by comparing the results obtained for the 10 K and 265 K supercells, was found to be negligible.

Using the data of Figs. 2(a) and 3 we now compute the average formation free energy G_f as a function of tem-

perature within the local-harmonic approximation. The results are shown in Fig. 2(b). A comparison between both interstitial configurations reveals that, coherent with the results in Fig. 2(a), the formation free energy of the Bc interstitial is found to be lower than that of the Tu structure across the entire temperature interval. Considering the formation free-energy difference between the vacancy and Bc interstitial, the downward shift of the vacancy curve with respect to the Bc interstitial compared to Fig. 2(a) is due to zero-point energy contributions, which lower the DFT vacancy formation energy by ~ 0.08 eV compared to a reduction of ~ 0.02 eV for the Bc interstitial. This implies that the vibrations of the Bc interstitial are more “bulklike” than the vacancy in that it contains only one molecule that is not fully hydrogen bonded, compared to the four in case of the vacancy. As the temperature increases, however, the formation free-energy difference between the defects decreases because of the high formation entropy of Bc interstitial. At $T = 265$ K, for instance, from the derivative of G_f with respect to temperature, the formation entropy of the Bc interstitial reaches a value of $\sim 7k_B$ compared to $\sim 5k_B$ for the vacancy. The origin of this elevated formation entropy value [5] is mostly associated with the appreciable reduction of the DFT formation energy contribution upon thermal expansion as shown in Fig. 2(a).

Finally, to evaluate the relative importance of the different point-defect species, we determine their thermal-equilibrium concentrations c (per crystal lattice site) as a function of temperature according to [1]

$$c = zN \exp(-G_f/k_B T), \quad (1)$$

where N is the number of available defect sites per lattice site and, for the interstitial defects, z represents the number of possible orientations of the interstitial molecule on a given site. For the Tu and Bc interstitials we have $N_{\text{Tu}} = 1/2$ and $N_{\text{Bc}} = 2$, respectively, which follows from the number of cages and the number of hydrogen bonds per lattice site [1]. For the Tu interstitial we have observed that the orientation of an interstitial molecule on a given Tu site is always such that both of its O-H bonds tend to closely align with two oxygen atoms of the surrounding cage. Within this assumption, counting the number of different ways in which this can be realized, taking into account the fact that the H-O-H angle of the interstitial molecule is approximately 104° , we deduce $z_{\text{Tu}} = 40$. From different realizations of the Bc interstitial on a given site we estimate $z_{\text{Bc}} = 4$. For instance, considering Fig. 1(c), a different stable orientation was obtained by rotating the interstitial molecule such that its dangling hydrogen-bond points along the c axis, out of the paper. Two more stable orientations with similar energies were then created by a mirror symmetry operation with respect to the plane containing the line connecting molecules 1 and 2 and the c axis. For the molecular vacancy we have $N_V = z_V = 1$.

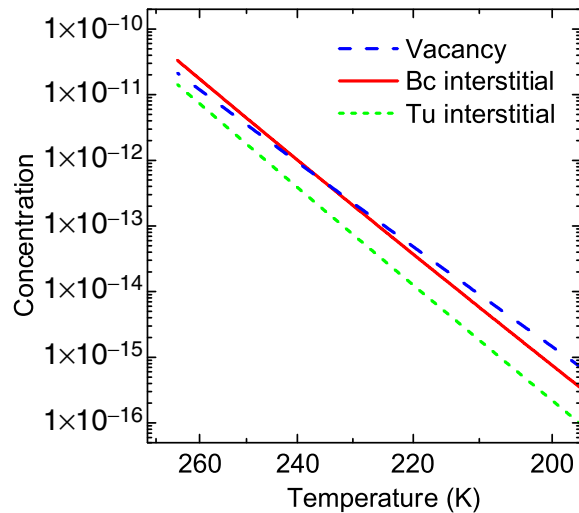


FIG. 4 (color online). Thermal-equilibrium concentrations as a function of temperature for the Tu interstitial (short dashed line), Bc interstitial (full line), and vacancy (dashed line).

Assuming these values for the site multiplicities, Fig. 4 shows the Arrhenius plot for the concentrations of the molecular vacancy and the Tu and Bc interstitials. It is found that the former is significantly lower than that of the latter across the entire temperature interval, supporting the view that a structure different from the established Tc and Tu interstitials is the preferred interstitial configuration in ice I_h . Indeed, given the structural properties of the Bc interstitial, this is coherent with the experimental suggestion of a bound self-interstitial [5]. Furthermore, the results indicate that the vacancy is the dominant point-defect species in ice I_h for temperatures below $T \sim 200$ K. However, due to the decreasing formation free-energy difference between the vacancy and Bc interstitial, the thermal-equilibrium concentrations of both defect species cross near $T \approx 230$ K. This is consistent with the crossover scenario suggested in Ref. [5], in which the interstitial is assumed to dominate for temperatures above -50°C whereas the vacancy becomes the principal thermal-equilibrium point defect at lower temperatures.

In summary, we present a DFT-based study of the structure and formation energetics of a series of molecular point defects in ice I_h . The results suggest that, due to its bonding to the surrounding hydrogen-bond network, the Bc interstitial is the favored molecular interstitial structure in ice I_h . Considering the equilibrium concentrations as a function of temperature, the molecular vacancy is found to be the favored molecular point defect for $T \lesssim 200$ K. Because of the high formation entropy of the Bc interstitial, however, a crossover scenario in which the Bc interstitial becomes favored at temperatures below the melting point is conceivable.

The authors gratefully acknowledge financial support from the Brazilian agencies FAPESP, CNPq, and CAPES. M. K. acknowledges R. W. Whitworth for stimulating discussions. Part of the calculations were carried out at the High-Performance Computing Facility at CCJDR-IFGW-UNICAMP.

*To whom correspondence should be addressed.

Email address: dekonig@ifi.unicamp.br

- [1] V. F. Petrenko and R. W. Whitworth, *The Physics of Ice* (Oxford University Press, Oxford, 1999).
- [2] C. Haas, *Phys. Lett.* **3**, 126 (1962).
- [3] O. E. Mogensen and M. Eldrup, *J. Glaciol.* **21**, 85 (1978).
- [4] M. Eldrup, O. E. Mogensen, and J. H. Bilgram, *J. Glaciol.* **21**, 101 (1978).
- [5] T. Hondoh, T. Itoh, and A. Higashi, in *Point Defects and Defect Interactions in Metals*, edited by J. Takamura, M. Doyama, and M. Kiritani (University of Tokyo Press, Tokyo, 1982), p. 599.
- [6] K. Goto, T. Hondoh, and A. Higashi, in *Point Defects and Defect Interactions in Metals*, edited by J. Takamura, M. Doyama, and M. Kiritani (University of Tokyo Press, Tokyo, 1982), p. 174.
- [7] K. Goto, T. Hondoh, and A. Higashi, *Jpn. J. Appl. Phys.* **25**, 351 (1986).
- [8] T. Hondoh, K. Azuma, and A. Higashi, *J. Phys. Paris* **48**, No. C1, 183 (1987).
- [9] M. Oguro and T. Hondoh, in *Lattice Defects in Ice Crystals*, edited by A. Higashi (Hokkaido University Press, Sapporo, 1988), p. 49.
- [10] N. H. Fletcher, *The Chemical Physics of Ice* (Cambridge University Press, Cambridge, England, 1970).
- [11] H. Itoh, K. Kawamura, T. Hondoh, and S. Mae, *J. Chem. Phys.* **105**, 2408 (1996).
- [12] A. Demurov, R. Radhakrishnan, and B. L. Trout, *J. Chem. Phys.* **116**, 702 (2002).
- [13] T. Ikeda-Fukazawa, S. Horikawa, T. Hondoh, and K. Kawamura, *J. Chem. Phys.* **117**, 3886 (2002).
- [14] M. de Koning, A. Antonelli, A. J. R. da Silva, and A. Fazzio, *Phys. Rev. Lett.* **96**, 075501 (2006).
- [15] G. Kresse and J. Hafner, *Phys. Rev. B* **47**, R558 (1993).
- [16] G. Kresse and J. Furthmüller, *Comput. Mater. Sci.* **6**, 15 (1996).
- [17] G. Kresse and D. Joubert, *Phys. Rev. B* **59**, 1758 (1999).
- [18] J. A. Hayward and J. R. Reimers, *J. Chem. Phys.* **106**, 1518 (1997).
- [19] M. Finnis, *Interatomic Forces in Condensed Matter* (Oxford University Press, New York, 2003), Chap. 5, pp. 156–157.
- [20] R. LeSar, R. Najafabadi, and D. J. Srolovitz, *Phys. Rev. Lett.* **63**, 624 (1989).
- [21] J.-C. Li and D. K. Ross, in *Physics and Chemistry of Ice*, edited by N. Maeno and T. Hondoh (Hokkaido University Press, Hokkaido, 1992), p. 27.